Scientia Iranica B (2021) 28(2), 757–772

Sharif University of Technology
Scientia Iranica
Transactions B: Mechanical Engineering
http://scientiairanica.sharif.edu

Gain-scheduled h_2/h_∞ autopilot design with regional pole placement constraints: An LMI-based approach

H. Behrouz, I. Mohammadzaman*, and A. Mohammadi

Faculty of Electrical Engineering, Malek Ashtar University of Technology, Tehran, P.O. Box 15875-1774, Iran.

Received 4 April 2019; received in revised form 20 November 2020; accepted 7 December 2020

KEYWORDS
Robust three-loop autopilot;
Mixed H_2/H_∞ control;
Regional pole placement;
Time-domain performance;
Gain-scheduled autopilot.

Abstract. In this paper, a gain-scheduled three-loop autopilot is designed for the pursuit system that can satisfy the mixed H_2/H_∞ performance and time-domain constraints. The gain-scheduled autopilot problem was first converted into a state-feedback control problem for Linear Parameter Varying (LPV) systems and then, a control method was proposed using the Linear Matrix Inequality (LMI) approaches. The new approaches could satisfy the mixed H_2/H_∞ performance and regional pole placement constraints and ensure no constraints on system matrices. The final gain-scheduled autopilot which can promise greater stability and performance for the entire parameter range was calculated using the interpolation of the finite number of fixed controllers. Simulation results showed the efficiency of the proposed method in designing the three-loop autopilot.

1. Introduction

The main objective of a pursuit autopilot is to track the commands received from the guidance computer with high performance [1]. To this end, the autopilot should provide a fast response to intercept an agile target as well as ensure the desired robustness under the effect of unmodeled dynamics, noises, and disturbances [2,3]. In fact, the pursuit model has a wide variation in its parameters. Accordingly, a robust autopilot that maintains stability and satisfies complicated constraints on the closed-loop response is a challenging control problem [4].

The pursuits can be modeled as a Linear Parameter-Varying (LPV) system with the autopilot design [5–7]. LPV systems are characterized by time-varying parameters and their controllers are generally scheduled in real time based on the measured parameters [8–10]. A robust gain-scheduled controller is usually applied to control LPV systems such as the robust Proportional-Integral-Derivative (PID) design [11,12], H_∞ controllers [13–16], linear fractional methods [17], and H_2 controllers with pole placement constraints [18]. These methods ensure both stability and performance through Linear Matrix Inequality (LMI) approaches [19]. Furthermore, the estimators can be used for identifying and canceling the disturbance and coupling effects on the pursuit dynamic [20–22].

It has been found that the mixed H_2/H_∞ control strategy is highly effective for robust purposes in the case of LPV systems under bounded external noise and disturbance inputs [23–29]. The mixed H_2/H_∞ methods combine the quadratic performance and disturbance attenuation. However, these methods typically offer a good transient response for an Linear Time Invariant (LTI) system, not LPV system. Therefore, a

*. *Corresponding author.*
E-mail address: iman_mz@yahoo.com (I. Mohammadzaman)

doi: 10.24200/sci.2020.53269.3154

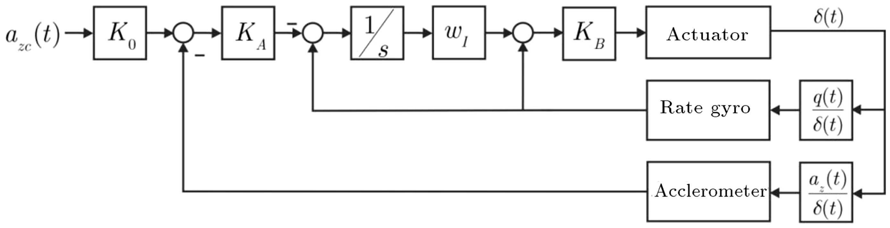

Figure 1. Block diagram of a standard three-loop autopilot.

good idea for designing a gain-scheduled controller is to combine robust methods with time-domain constraints (i.e., the pole placement) [30]. The gain-scheduled methods that ensure time-domain characteristics for LPV systems can be found in [31,32]. However, the methods suggested in [31,32] cannot materialize high robust performance. In [28], the mixed H_2/H_∞ performances and closed-loop poles constraints were taken into account to study the problem of state-feedback controller design for an LPV. However, it was assumed that the input matrices needed to be fixed. Therefore, the method given in [28] cannot be applied to a pursuit model because the input matrix of the pursuit model is generally non-fixed. In this paper, the problem of designing the LPV state feedback controller without any constraints on system matrices was studied to achieve robustness and stimulate the desired closed-loop time-domain response. Furthermore, the mixed H_2/H_∞ control strategy and regional pole constraints were applied. The novelty of the proposed method lies in its applicability to designing a gain-scheduled autopilot for a pursuit system. The proposed controller is static and scheduled in real time by the interpolation of the fixed static controllers in every vertex of the parameter box. In addition, the interpolation technique of the proposed method utilizes the convex concept to guarantee the robustness and performance of the closed-loop LPV system. Furthermore, the static LTI controllers are designed offline and then, interpolated in real time using the measured parameters. Therefore, it has simple implementation with respect to the dynamic gain-scheduling controllers.

An autopilot can be designed based on feedback topology from the normal acceleration and angular velocity that are nominated as two-loop autopilots [33]. Nevertheless, a good structure called standard three-loop autopilot was proposed in [34,35]. The three-loop structure is faster than the two-loop one in terms of tracking acceleration. Furthermore, it is more robust than the two-loop topology [36]. As shown in Figure 1, in the three-loop topology, the deflection angle is calculated from the weighted error acceleration, angular velocity, and integral of angular velocity [37]. The integral of angular velocity is used to increase the stability margin [35]. This configuration guarantees high performance and robustness; therefore, it is appropriate that a pursuit system should be controlled by different parameters [35]. Several methods have been proposed to design and consider the standard three-loop autopilot in [38–41] in which the pursuit system was considered as an LTI system and the autopilot could not guarantee the stability of the LPV system. However, in this paper, the nonlinear pursuit system was converted into an LPV model. Then, the gain-scheduled controller was calculated through the LMI technique. The main objective of this study is to propose a method to obtain the static autopilot gains, as shown in Figure 1.

In addition, this paper contributes to converting the standard three-loop autopilot problem into a standard state-feedback problem. Therefore, the pursuit model is considered an LPV system to propose the gain-scheduled static state-feedback controller that can guarantee both H_2/H_∞ performance and regional pole constraint. Finally, this method is employed to calculate the three-loop gains and their efficiency was illustrated through simulation results.

This paper is organized as follows. In Section 2, the preliminaries, notation, and definitions are presented. In Section 3, the LPV mathematical model of the conventional pursuit and the procedure of converting the problem of the standard three-loop autopilot into the state feedback control formulation are described. Then, the static gain-scheduled controller design is explained in Section 4. Finally, in Section 5, the proposed techniques are discussed to calculate the three-loop autopilot gains and the obtained simulation results are presented.

2. Preliminaries, notation, and definitions

Consider a continuous-time polytopic system described by the following state-space equations:

$$\dot{x}(t) = A(\theta(t))\,x(t) + B_1(\theta(t))\,w(t)$$

$$+B_2(\theta(t))\,u(t),$$

$$z_\infty(t) = C_1(\theta(t))\,x(t) + D_{11}(\theta(t))\,w(t)$$

$$+D_{12}(\theta(t))\,u(t),$$

$$z_2(t) = C_2(\theta(t))\,x(t) + D_{22}(\theta(t))\,u(t),$$

$$y(t) = x(t), \tag{1}$$

where $x(t)$ is the state vector, $u(t)$ is the control input, $w(t)$ is the exogenous input or the unknown disturbance input, and $z_\infty(t)$ and $z_2(t)$ are the controlled outputs. The main objective of this paper was to design the three-loop autopilot in order that the closed-loop pursuit system (Eq. (1)) would satisfy the following conditions:

1. The closed-loop poles are located in the desired region of the complex plane.
2. The performances of H_2 and H_∞ are simultaneously guaranteed or:

$$\|T_\infty\|_\infty = \left\|\frac{z_\infty(t)}{w(t)}\right\|_\infty < \gamma,$$

$$\|T_2\|_2 = \left\|\frac{z_2(t)}{w(t)}\right\|_2 < \gamma. \tag{2}$$

Remark 1. The H_2 control problem stabilizes the system internally and minimizes the H_2 norm. By minimizing the H_2 norm of the system, both the control inputs and state variables can be controlled [42]. Therefore, the H_2 performance guarantees good performance of the closed-loop system by imposing limitation on control and state signals [43]. However, H_∞ control is to find an admissible controller such that the infinity norm of the transfer function $T_{z_\infty w}$ can be minimized [42]. Equivalently, the H_∞ control problem is used to enhance the robustness of the design [43]. Therefore, the mixed H_2/H_∞ control is used to achieve higher design robustness as well as better performance on the control and state signals.

In the following, some required preliminary lemmas are given.

Definition 1 [44]. The parameter dependence is affine. In other words, the state space matrices of the system, $\{A(\theta(t)), B(\theta(t)), C(\theta(t)), D(\theta(t))\}$, can be written as affine in terms of $\theta(t)$. Polytope is a convex hull of a finite number of matrices N_i with similar dimensions, i.e.:

$$Co\{N_i : i = 1, 2, ..., r\} := \left\{\sum_{i=1}^{r} \alpha_i N_i : \alpha_i \geq 0, \sum_{i=1}^{r} \alpha_i = 1\right\}. \tag{3}$$

Definition 2 [45]. Time-varying parameter $\theta(t)$ varies according to the vertices, $(\theta_1, \theta_1, ..., \theta_r)$, in a polytope,

$$\theta(t) \in \Theta := Co\{\theta_1, \theta_1, ..., \theta_r\} = \left\{\sum_{i=1}^{r} \alpha_i \theta_i : \alpha_i \geq 0, \sum_{i=1}^{r} \alpha_i = 1\right\}. \tag{4}$$

The vertices show the external values for the parameters. The state-space matrix of the system whose parameters change in a polytope is a polytopic system, i.e.:

$$\begin{pmatrix} A(\theta(t)) & B(\theta(t)) \\ C(\theta(t)) & D(\theta(t)) \end{pmatrix} \in Co \left\{\begin{pmatrix} A_i & B_i \\ C_i & D_i \end{pmatrix} : i = 1, 2, ..., r\right\},$$

$$\begin{pmatrix} A_i & B_i \\ C_i & D_i \end{pmatrix} := \begin{pmatrix} A(\theta_i) & B(\theta_i) \\ C(\theta_i) & D(\theta_i) \end{pmatrix}, \theta(t) \in \Theta. \tag{5}$$

Lemma 1. Consider the LTI system described by:

$$\dot{x}(t) = A_{cl}x(t) + B_{cl}w(t),$$

$$z(t) = C_{cl}x(t) + D_{cl}w(t), \tag{6}$$

where $x(t)$ is the state, $w(t)$ is the exogenous input, $z(t)$ is the controlled output, and A_{cl} is stability. By defining the transfer function $T(s)$ of realization as $T(s) = C_{cl}(sI - A_{cl})^{-1}B_{cl} + D_{cl}$ and the symmetric positive definite matrices X_1 and X_2, $\|T(s)\|_\infty \leq \gamma_1$ if and only if there exists X_1 such that the following inequality holds:

$$\begin{pmatrix} A_{cl}^T X_1 + X_1 A_{cl} & * & * \\ B_{cl}^T X_1 & -\gamma_1 I & * \\ C_{cl} & D_{cl} & -\gamma_1 I \end{pmatrix} < 0, \tag{7}$$

and $\|T(s)\|_2 \leq \gamma_2$ if and only if there exist X_2 and the auxiliary variable Z so that the following LMIs are feasible:

$$D_{cl} = 0, \begin{pmatrix} A_{cl}^T X_2 + X_2 A_{cl} & * \\ B_{cl}^T X_2 & -\gamma_2 I \end{pmatrix} < 0,$$

$$\begin{pmatrix} X_2 & * \\ C_{cl} & Z \end{pmatrix} > 0, \quad trace(Z) < \gamma_2. \tag{8}$$

Lemma 2 [45]. Consider the closed-loop system $\dot{x}(t) = \tilde{A}\,x(t)$. The eigenvalues of the system matrix $\tilde{A} \in \Re^{n\times n}$ are in the LMI region:

$$\left\{s \in C \left| \begin{pmatrix} I \\ sI \end{pmatrix}^* \begin{pmatrix} Q & * \\ S^T & R \end{pmatrix} \begin{pmatrix} I \\ sI \end{pmatrix} < 0 \right.\right\}, \tag{9}$$

if and only if there exists a definite solution $X > 0$ such that:

$$\begin{pmatrix} I \\ \tilde{A}\otimes I \end{pmatrix}^* \begin{pmatrix} X\otimes Q & * \\ X\otimes S^T & X\otimes R \end{pmatrix} \begin{pmatrix} I \\ \tilde{A}\otimes I \end{pmatrix} < 0, \tag{10}$$

where $P := \begin{pmatrix} Q & S \\ S^T & R \end{pmatrix}$ is the given LMI region in the complex plane, matrix I is an identity matrix, and $\otimes$ is the Kronecker product. By applying this lemma, the pole placement problem in the desired region of the complex plane would be transformed into LMI problems. In Table A.1 of Appendix A, some standard regions of the complex plane that can be converted to the LMI formulation are presented.

Remark 2. Lemmas 1 and 2 that can guarantee the quadratic performance of an LPV system are employed to derive LMI conditions for designing a gain-scheduled autopilot. The quadratic performance is equivalent to internal stability of an LPV system if there exists a fixed quadratic Lyapunov function for the entire parameter range [28,44]. Therefore, the Lyapunov matrices X_1, X_2, and X are assumed fixed.

Lemma 3 [45]. The matrix F has affine dependency in terms of x as follows:

$$F\left(x\right)=\begin{pmatrix}F_{11}\left(x\right) & F_{12}\left(x\right)\\ F_{21}\left(x\right) & F_{22}\left(x\right)\end{pmatrix}<0, \tag{11}$$

where $F_{11}(x)$ and $F_{22}(x)$ are square matrix. $F(x)$ is negative definite if and only if:

$$\begin{cases} F_{22}\left(x\right)<0\\ F_{22}\left(x\right)-F_{21}\left(x\right)\left(F_{11}\left(x\right)\right)^{-1}F_{12}\left(x\right)<0\end{cases} \tag{12}$$

or:

$$\begin{cases} F_{22}\left(x\right)<0\\ F_{11}\left(x\right)-F_{12}\left(x\right)\left(F_{22}\left(x\right)\right)^{-1}F_{21}\left(x\right)<0\end{cases} \tag{13}$$

Through this lemma, the nonlinear matrix inequalities (12) or (13) can be converted into LMI (Eq. (11)). This lemma is known by Schur complement lemma.

Lemma 4 [45]. If matrix M is a square and W is nonsingular, the product of W^*MW is a congruence transformation of the matrix M. For Hermitian matrix M, this transformation does not change the number of positive and negative eigenvalues of M. Indeed, if $M<0$, $W^*MW<0$, and vice versa.

3. The pursuit model and its application to designing a standard three-loop autopilot

In [46], a pursuit system was modeled using the perturbation method. In this model, while the roll-stabilized system is taken into account, the coupling effects among channels were ignored; in addition, the pursuit dynamics, roll, yaw, and pitch channels are separately considered and the equation of each axis is obtained. This paper aimed to provide the autopilot design over the pitch axis. The model of the pitch channel is given by:

$$\begin{bmatrix}\dot{\alpha}\left(t\right)\\ \dot{q}\left(t\right)\end{bmatrix}=\begin{bmatrix}-\frac{N_\alpha}{V(t)} & 1\\ M_\alpha & M_q\end{bmatrix}\begin{bmatrix}\alpha\left(t\right)\\ q\left(t\right)\end{bmatrix}+\begin{bmatrix}-\frac{N_\delta}{V(t)}\\ M_\delta\end{bmatrix}\delta\left(t\right),$$

$$a_z\left(t\right)=\begin{bmatrix}N_\alpha & 0\end{bmatrix}\begin{bmatrix}\alpha\left(t\right)\\ q\left(t\right)\end{bmatrix}+\left[N_\delta\right]\delta\left(t\right), \tag{14}$$

where $q(t)$, $\alpha(t)$, $\delta(t)$, and $a_z(t)$ are the pitch rate, angle of attack, deflection of pitch control, and normal acceleration, respectively. M and N denote the moment and forces applied to the pursuit, respectively. The dimensional derivatives N_α, N_δ, M_α, M_a, and M_δ are given in proportion to the non-dimensional derivatives $C_{m\alpha}$, $C_{N\delta}$, $C_{N\alpha}$, C_{mq}, and $C_{m\delta}$ by:

$$N_\alpha=\frac{\bar{q}S}{m}C_{N\alpha},\qquad N_\delta=\frac{\bar{q}S}{m}C_{N\delta},$$

$$M_\alpha=\frac{\bar{q}Sd}{Iy}C_{m\alpha},\qquad M_q=\frac{\bar{q}Sd^2}{2I_yV\left(t\right)}C_{mq},$$

$$M_\delta=\frac{\bar{q}Sd}{Iy}C_{m\delta}, \tag{15}$$

where $V(t)$, d, S, m, I_y, and $\bar{q}$ are the velocity, pursuit diameter, maximum cross-section, pursuit mass, moment of inertia, and dynamic pressure, respectively. ρ is the air density obtained by:

$$\bar{q}=\frac{1}{2}\rho V^2\left(t\right). \tag{16}$$

Based on Eqs. (14)–(16) and the height appearing indirectly in the model due to the parameter ρ, the pursuit is considered a model that varies according to flying conditions such as velocity and height. The autopilot structure in Figure 1 is a state feedback controller. In this respect, the block diagram shown in Figure 1 is added to System Model (14) and then, the closed-loop system is represented, as shown in Figure 2.

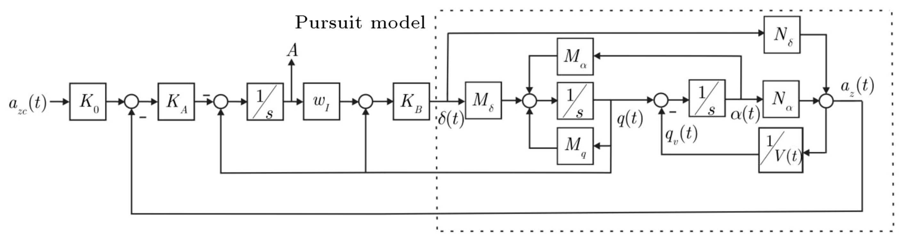

Figure 2. Block diagram of a standard three-loop autopilot with the pursuit model.

For the closed-loop system shown in Figure 2, the gain K_0, used for achieving DC gain 1, can easily be calculated as follows:

$$K_0 = \left(1 + \frac{1}{K_A\,V\,(t)}\right). \tag{17}$$

According to Eq. (17), using the three-loop structure enjoys an advantage, i.e., independency of the gain K_0 from the pursuit system. The value of pursuit velocity, $V(t)$, is large and if the gain is large enough, the gain $K_A V(t)$ in the command acceleration can be ignored. According to Figure 2, by defining $q_v\,(t) \triangleq \frac{a_z(t)}{V(t)}$, the point A is:

$$\begin{aligned} A &= \frac{K_A\,(a_z\,(t) - K_0 a_{zc}\,(t)) + q\,(t)}{s} \\ &= \frac{-K_0 K_A a_{zc}\,(t) + K_A\,q_v\,(t)\,V\,(t) + q\,(t)}{s}. \end{aligned} \tag{18}$$

Also, Eq. (18) can be rewritten into:

$$\begin{aligned} A = \frac{-K_0 K_A a_{zc}\,(t)}{s} + \frac{K_A\,q_v\,(t)\,V\,(t)}{s} \\ \left(1 + \frac{1}{K_A\,V\,(t)}\right) + \frac{q\,(t) - q_v\,(t)}{s}. \end{aligned} \tag{19}$$

Now, given that $\dot{\alpha}\,(t) = q\,(t) - q_v\,(t)$ in the block diagram of the closed-loop system shown in Figure 2, Eq. (19) will be:

$$\begin{aligned} A &= \frac{-K_0 K_A a_{zc}\,(t)}{s} + \frac{K_A\,q_v\,(t)\,V\,(t)}{s} \\ &\left(1 + \frac{1}{K_A\,V\,(t)}\right) + \frac{\dot{\alpha}\,(t)}{s} = \frac{-K_0 K_A a_{zc}\,(t)}{s} \\ &+ \frac{K_A\,q_v\,(t)\,V\,(t)}{s}\left(1 + \frac{1}{K_A\,V\,(t)}\right) + \alpha\,(t) \\ &= \frac{-K_0 K_A a_{zc}\,(t)}{s} + \frac{K_A\,a_z\,(t)}{s} \\ &\left(1 + \frac{1}{K_A\,V\,(t)}\right) + \alpha\,(t). \end{aligned} \tag{20}$$

Hence, from Eq. (20), Figure 2 can be incorporated in Figure 3.

Suppose that the gain of $K_A V(t)$ in Figure 3 is large; then, the gain $1 + \frac{1}{K_A\,V(t)}$ would be almost equal to one and Figure 4 can be derived from Figure 3 through simple mathematical operations, where:

$$K_q = K_B, \quad K_\alpha = K_B W_I, \quad K_z = K_A K_B W_I. \tag{21}$$

In Figure 4, the standard three-loop autopilot is a state feedback controller with an integrator in the acceleration path to remove the tracking error. In the following, the design procedure of the state space of the open-loop system is presented. Based on the block diagram of Figure 4, the state space of the open-loop system is described by:

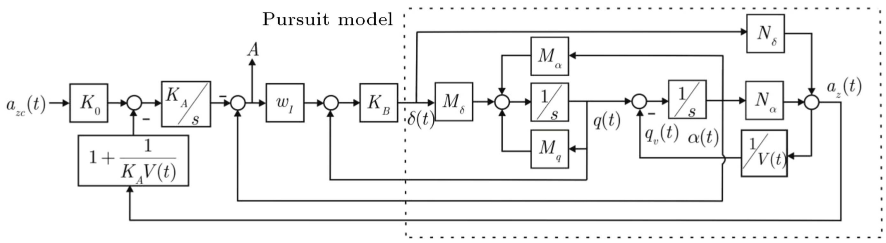

Figure 3. Reconstruction of the standard three-loop autopilot with the system model.

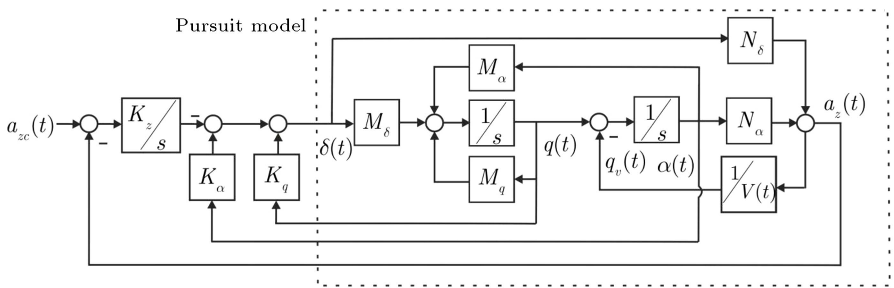

Figure 4. Block diagram of the pursuit system and the state feedback in the standard form.

$$\begin{bmatrix}\dot{\alpha}(t)\\ \dot{q}(t)\\ \dot{x}_z(t)\end{bmatrix}=\begin{bmatrix}-\frac{N_\alpha}{V(t)} & 1 & 0\\ M_\alpha & M_q & 0\\ N_\alpha & 0 & 0\end{bmatrix}\begin{bmatrix}\alpha(t)\\ q(t)\\ x_z(t)\end{bmatrix}$$

$$+\begin{bmatrix}-\frac{N_\delta}{V(t)}\\ M_\delta\\ N_\delta\end{bmatrix}\delta(t),$$

$$\begin{bmatrix}y_1(t)\\ y_2(t)\\ y_3(t)\end{bmatrix}=\begin{bmatrix}1 & 0 & 0\\ 0 & 1 & 0\\ 0 & 0 & 1\end{bmatrix}\begin{bmatrix}\alpha(t)\\ q(t)\\ x_z(t)\end{bmatrix}, \tag{22}$$

where $x_z(t)$ is a state variable obtained from the integrator element. By designing the controller for the state-space model (Eq. (22)), the following controller will be achieved:

$$\delta(t)=\begin{bmatrix}K_\alpha & K_q & K_z\end{bmatrix}\begin{bmatrix}\alpha(t)\\ q(t)\\ x_z(t)\end{bmatrix}. \tag{23}$$

As a result, if the state feedback controller (Eq. (23)) is designed for the open-loop system (Eq. (22)), the standard three-loop autopilot can be implemented by Eq. (21), as shown in Figure 2. The following discusses how similar the nonlinear tail-controlled pursuit model given by Nichols et al. [47] is to the presented state-space model (Eq. (14)) and whether it can be modeled as an LPV system. The pursuit model is taken from [47]:

$$\dot{\alpha}(t)=K_\alpha M(t)\,C_n(\alpha(t),\delta(t),M(t))\cos(\alpha(t))$$

$$+q(t),$$

$$\dot{q}(t)=K_q M^2(t)\,C_m(\alpha(t),\delta(t),M(t)),$$

$$a_z(t)=K_z M^2(t)\,C_n(\alpha(t),\delta(t),M(t)), \tag{24}$$

where the variables $a_z(t)$ and $q(t)$ can be measured using accelerometer and gyroscope, and the aerodynamic coefficients are defined by:

$$C_n(\alpha(t),\delta(t),M(t))=sign(\alpha(t))$$

$$\left[a_n|\alpha(t)|^3+b_n|\alpha(t)|^2+c_n\left(2-\frac{M(t)}{3}\right)|\alpha(t)|\right]$$

$$+d_n\delta(t),$$

$$C_m(\alpha(t),\delta(t),M(t))=sign(\alpha(t))$$

$$\left[a_m|\alpha(t)|^3+b_m|\alpha(t)|^2+c_m\left(-7+\frac{8M(t)}{3}\right)|\alpha(t)|\right]$$

$$+d_m\delta(t), \tag{25}$$

where $M(t)$ is the Mach number. Model (24) presents a pursuit model at an altitude of 2000ft and the values for the parameters in Eqs. (24) and (25) are presented in Table B.1. For design purposes, in the following, first, the similarity of the nonlinear Model (24) to Model (14) is elaborated. To this end, the following can be substituted:

$$sign(\alpha(t))\,|\alpha(t)|,$$

$$M(t)=\frac{V(t)}{\nu_s}, \tag{26}$$

where v_s is the speed of sound and the aerodynamic coefficients (Eq. (25)) can be rewritten as:

$$C_n(\alpha(t),\delta(t),M(t))=\left[a_n|\alpha(t)|^2+b_n|\alpha(t)|\right.$$

$$\left.+c_n\left(2-\frac{M(t)}{3}\right)\right]\alpha(t)+d_n\delta(t),$$

$$=\tilde{C}_n\,\alpha(t)+d_n\delta(t)$$

$$C_m(\alpha(t),\delta(t),M(t))=\left[a_m|\alpha(t)|^2+b_m|\alpha(t)|\right.$$

$$\left.+c_m\left(-7+\frac{8M(t)}{3}\right)\right]\alpha(t)+d_m\delta(t)$$

$$=\tilde{C}_m\,\alpha(t)+d_m\delta(t). \tag{27}$$

By using the aerodynamics parameters (Eq. (27)) and assuming the angle of attack being small, the pursuit system (Eq. (24)) is obtained as:

$$\begin{bmatrix}\dot{\alpha}(t)\\ \dot{q}(t)\end{bmatrix}=\begin{bmatrix}K_\alpha M(t)\,\tilde{C}_n & 1\\ K_q M^2(t)\,\tilde{C}_m & 0\end{bmatrix}\begin{bmatrix}\alpha(t)\\ q(t)\end{bmatrix}$$

$$+\begin{bmatrix}K_\alpha M(t)\,d_n\\ K_q\,M^2(t)\,d_m\end{bmatrix}\delta(t),$$

$$a_z(t)=\begin{bmatrix}K_z M^2(t)\,\tilde{C}_n & 0\end{bmatrix}\begin{bmatrix}\alpha(t)\\ q(t)\end{bmatrix}$$

$$+\begin{bmatrix}K_z M^2(t)\,d_n\end{bmatrix}\delta(t), \tag{28}$$

or:

$$\begin{bmatrix}\dot{\alpha}(t)\\ \dot{q}(t)\end{bmatrix}=\begin{bmatrix}-\frac{N_\alpha}{V(t)} & 1\\ M_\alpha & 0\end{bmatrix}\begin{bmatrix}\alpha(t)\\ q(t)\end{bmatrix}$$

$$+\begin{bmatrix}-\frac{N_\delta}{V(t)}\\ M_\delta\end{bmatrix}\delta(t),$$

$$A_z(t)=\begin{bmatrix}N_\alpha & 0\end{bmatrix}\begin{bmatrix}\alpha(t)\\ q(t)\end{bmatrix}+[N_\delta]\,\delta(t), \tag{29}$$

with:

$$N_\alpha = -K_z M^2(t)\,\tilde{C}_n, N_\delta = -K_z M^2(t)\,d_n,$$

$$M_\alpha = K_q M^2(t)\,\tilde{C}_m, M_\delta = K_q M^2(t)\,d_m,$$

$$K_z = K_\alpha \nu_s, \qquad A_z(t) = -a_z(t). \tag{30}$$

According to Eq. (29), the pursuit model (Eq. (24)) is similar to System (14). Therefore, the problem of the standard three-loop autopilot design is equivalent to a state feedback controller technique that can be applied for System (29) and then, implemented as the standard three-loop structure. Now, the model is converted into an LPV model. If $|\alpha(t)| \leq 20^\circ$ and $1 \leq M(t) \leq 2.5$, by defining the following parameters:

$$\theta_1 = K_q M^2(t)\left[a_m|\alpha(t)|^2 + b_m|\alpha(t)| + c_m\left(-7 + \frac{8M(t)}{3}\right)\right],$$

$$\theta_2 = M^2(t), \tag{31}$$

the space model in Eq. (29) can be modeled using the least square optimization technique, as shown in the following LPV system:

$$\begin{bmatrix}\dot{\alpha}(t)\\ \dot{q}(t)\end{bmatrix} = \begin{bmatrix}A_{11}\theta_1(t) + A_{12}\theta_2(t) & 1\\ A_{21}\theta_1(t) & 0\end{bmatrix}\begin{bmatrix}\alpha(t)\\ q(t)\end{bmatrix} + \begin{bmatrix}B_{11}\theta_2(t) + B_{12}\\ B_{21}\theta_2(t)\end{bmatrix}\delta(t),$$

$$A_z(t) = \begin{bmatrix}C_{11}\theta_1(t) + C_{12}\theta_2(t) & 0\end{bmatrix}\begin{bmatrix}\alpha(t)\\ q(t)\end{bmatrix} + \left[D_{11}\theta_2(t)\right]\,\delta(t), \tag{32}$$

where:

$$A_{11} = 0.58, \quad A_{21} = 57.29, \quad B_{11} = -0.0098,$$

$$C_{11} = 14, \quad D_{11} = -1.3, \quad A_{12} = -0.031,$$

$$B_{21} = -14.54, \quad B_{12} = -0.037, \quad C_{12} = -7.4. \tag{33}$$

Table 1 shows the system units. Model (32) can be used for autopilot design in Section 5.

However, since the pursuit model is an LPV model, it is necessary to derive a controller to achieve better stability and performance for the system parameters. In the next section, the procedure of the controller design (Eq. (23)) for the LPV system (Eq. (22)) is elaborated in detail.

Table 1. Units of the model variables.

$\alpha(t)$	$q(t)$	$\delta(t)$	$A_z(t)$
rad	rad/sec	rad	g

4. Gain-scheduled H_2/H_∞ design with regional pole placement constraints

In this section, the gain-scheduled static state feedback is proposed by implementing the mixed H_2/H_∞ performance and time-domain constraints and taking the open-loop LPV system (Eq. (1)) into consideration.

Theorem 1. Consider the LPV System (Eq. (1)). There exists a gain-scheduled static controller that guarantees the quadratic H_2/H_∞ index γ and the time-domain specification if and only if matrices $L = L^T$, Z_2, and $\forall\ i = 1, 2, ..., r$ exist such that:

$$L > 0,$$

$$\phi_{ii} < 0, \qquad i = 1, 2, ..., r,$$

$$\phi_{ij} + \phi_{ji} < 0, \qquad i < j = 1, 2, ..., r, \tag{34}$$

$$\omega_{ii} < 0, \qquad i = 1, 2, ..., r,$$

$$\omega_{ij} + \omega_{ji} < 0, \qquad i < j = 1, 2, ..., r,$$

$$\Psi^k_{ii} < 0, \qquad i = 1, 2, ..., r, \qquad k = 1, 2,$$

$$\Psi^k_{ij} + \Psi^k_{ji} < 0, \quad i < j = 1, 2, ..., r, \quad k = 1, 2,$$

$$trace(Z_2) < \gamma, \tag{35}$$

where ϕ_{ij}, ω_{ij}, Ψ^1_{ij}, and Ψ^2_{ij} are calculated by Eqs. (36) and (37) as shown in Box I.

$$P := \begin{pmatrix}Q & S\\ S^T & R\end{pmatrix}, \quad R \triangleq T, \quad U^{-1}T^T, \quad U > 0 \tag{38}$$

represents the desired time-domain constraints. Then, the fixed controllers are readily obtained in every vertex as follows:

$$K_i = Y_i L^{-1}, \quad \forall i = 1, 2, ..., r. \tag{39}$$

Finally, the following polytopic LPV controller is proposed:

$$K = \sum_{i=1}^{r}\alpha_i K_i, \alpha_i \geq 0, \sum_{i=1}^{r}\alpha_i = 1, \tag{40}$$

where α_i satisfying Eq. (40) must be calculated in real time by the measured parameters.

Proof. First, the gain-scheduled static controller that guarantees the time-domain constraints is proved and then, its mixed H_2/H_∞ performance is added. Given the open-loop system (Eq. (1)) with $w(t) = 0$ through Lemma 2 and the control input $u(t) = K(\theta(t))\,x(t)$, the eigenvalues of the closed-loop system, $\tilde{A}(\theta(t)) = A(\theta(t)) + B_2(\theta(t))\,K(\theta(t))$, are located on the defined complex plane by Matrix P if and only if there exists

$$\phi_{ij} = \begin{pmatrix} L\otimes Q + (A_iL\otimes S + B_{2j}Y_i\otimes S)^T + (A_iL\otimes S + B_{2j}Y_i\otimes S) & * \\ A_iL\otimes T^T + B_{2j}Y_i\otimes T^T & -L\otimes U \end{pmatrix}, \tag{36}$$

$$\omega_{ij} = \begin{pmatrix} (A_iL + B_{2j}Y_i)^T + (A_iL + B_{2j}Y_i) & * & * \\ B_{1i}^T & -\gamma I & * \\ C_{1i}L + D_{12j}Y_i & D_{11i} & -\gamma I \end{pmatrix},$$

$$\Psi_{ij}^1 = \begin{pmatrix} (A_iL + B_{2j}Y_i)^T + (A_iL + B_{2j}Y_i) & * \\ B_{1i}^T & -\gamma I \end{pmatrix},$$

$$\Psi_{ij}^2 = -\begin{pmatrix} L & * \\ C_{1i}L + D_{22j}Y_i & Z_2 \end{pmatrix}. \tag{37}$$

Box I

a matrix $X > 0$ so that the matrix Inequality (10) can be feasible. Matrix Inequality (10) is equivalent to:

$$X\otimes Q + \left(X\tilde{A}(\theta(t))\right)^T \otimes S^T + \left(X\tilde{A}(\theta(t))\right)\otimes S + \left(\tilde{A}^T(\theta(t))X\tilde{A}(\theta(t))\right)\otimes R < 0. \tag{41}$$

This inequality is nonlinear due to $\tilde{A}(\theta(t))$. Therefore, first, this inequality is regarded as a linear inequality of $\tilde{A}(\theta(t))$. By assuming $R \geq 0$ and the properties of Kronecker product as:

$$(A\otimes B)(C\otimes D)(E\otimes F) = (ACE\otimes BDF). \tag{42}$$

the nonlinear term in Eq. (41), $\tilde{A}^T(\theta(t))\ X\tilde{A}(\theta(t))$, is:

$$\left(\tilde{A}^T(\theta(t))X\tilde{A}(\theta(t))\right)\otimes R = \tilde{A}\left(^T(\theta(t))XX^{-1}X\tilde{A}(\theta(t))\right)\otimes R = \left(\tilde{A}^T(\theta(t))X\otimes T\right)(X\otimes U)^{-1} \left(X\tilde{A}(\theta(t))\otimes T^T\right). \tag{43}$$

Then, by using Eq. (43) and Schur complement, Inequality (41) is:

$$\begin{pmatrix} N_1 & * \\ X(A(\theta(t)) + B_2(\theta(t))K(\theta(t)))\otimes T^T & -X\otimes U \end{pmatrix} < 0, \tag{44}$$

where:

$$N_1 = X\otimes Q + (X(A(\theta(t)) + B_2(\theta(t))K(\theta(t))))^T \otimes S^T + X(A(\theta(t)) + B_2(\theta(t))K(\theta(t)))\otimes S. \tag{45}$$

Now, an LMI formulation is required to evaluate the controller in each of the parameter vertices. Therefore, through the congruence transformation with the matrix W as:

$$W = \begin{pmatrix} X^{-1}\otimes I & 0 \\ 0 & X^{-1}\otimes I \end{pmatrix}, \tag{46}$$

and Lemma 4, Matrix Inequality (44) is equal to:

$$N = \begin{pmatrix} N_{11} & * \\ N_{12}^T & N_{22} \end{pmatrix} < 0, \tag{47}$$

where:

$$N_{11} = X^{-1}\otimes Q + X^{-1}A^T(\theta(t))\otimes S^T + X^{-1}(B_2(\theta(t))K(\theta(t)))^T \otimes S^T + A(\theta(t))X^{-1}\otimes S\ + B_2(\theta(t))K(\theta(t))X^{-1} \otimes S,$$

$$N_{12} = X^{-1}A^T(\theta(t))\otimes T + X^{-1}(B_2(\theta(t))K(\theta(t)))^T \otimes T,$$

$$N_{22} = -X^{-1}\otimes U. \tag{48}$$

Now, by considering the polytopic system (Eq. (1)) with $w(t) = 0$, Controller (39), and the change of variables, we have:

$$L = X^{-1},$$

$$Y_i = K_iL, \quad \forall i = 1, 2, ..., r. \tag{49}$$

Inequality (47) is equivalent to the following LMI's.

$$\sum_{i=1}^{r}\sum_{j=1}^{r}\alpha_i\alpha_j\phi_{ij} < 0, \tag{50}$$

where ϕ_{ij} is given in Eq. (36). LMIs (50) are satisfied in case of the feasibility of Eq. (34). Therefore, the time-domain performance can be ensured by Inequalities (34). In the following, Robust Inequalities (35) will be proved. In this regard, through the augmented system (Eq. (1)) and Lemma 1, the H_2/H_∞ constraints are satisfied if and only if Inequalities (7) and (8) are feasible. Equivalently, controller $K(\theta(t))$ guarantees the H_2/H_∞ constraints instantaneously by the quadratic performance $\gamma = \gamma_1 = \gamma_2$ if there exists a symmetric positive definite matrix $X = X_1 = X_2$. Let $u(t) = K(\theta(t))\, x(t)$; therefore, Inequalities (7) and (8) can be presented as follows:

$$\begin{pmatrix} M_{11} & * & * \\ B_1^T(\theta(t))\, X & -\gamma I & * \\ C_1(\theta(t)) + D_{12}(\theta(t))\, K(\theta(t)) & D_{11}(\theta(t)) & -\gamma I \end{pmatrix} < 0, \tag{51}$$

$$\begin{pmatrix} M_{11} & * \\ B_1^T(\theta(t))\, X & -\gamma I \end{pmatrix} < 0$$

$$-\begin{pmatrix} X & * \\ C_2(\theta(t)) + D_{22}(\theta(t))\, K(\theta(t)) & Z_2 \end{pmatrix} < 0$$

$$trace\,(Z_2) < \gamma, \tag{52}$$

where:

$$M_{11} = \left(A(\theta(t)) + B_2(\theta(t))\, K(\theta(t))\right)^T X$$
$$+ X\left(A(\theta(t)) + B_2(\theta(t))\, K(\theta(t))\right). \tag{53}$$

Inequalities (51) and (52) are nonlinear with respect to $K(\theta(t))$ and X. Now, by applying the congruence transformation of Inequalities (51) and (52) with:

$$W_\infty = \begin{pmatrix} X^{-1} & 0 & 0 \\ 0 & I & 0 \\ 0 & 0 & I \end{pmatrix},$$

$$W_2 = \begin{pmatrix} X^{-1} & 0 \\ 0 & I \end{pmatrix}, \tag{54}$$

and by considering the polytopic system (Eq. (1)), Controller (39), and the change of variables (Eq. (49)), these inequalities will be as follows:

$$\sum_{i=1}^{r}\sum_{j=1}^{r} \alpha_i \alpha_j \omega_{ij} < 0, \qquad \sum_{i=1}^{r}\sum_{j=1}^{r} \alpha_i \alpha_j \Psi_{ij}^1 < 0,$$

$$\sum_{i=1}^{r}\sum_{j=1}^{r} \alpha_i \alpha_j \Psi_{ij}^2 < 0, \qquad trace\,(Z_2) < \gamma, \tag{55}$$

ω_{ij} , Ψ_{ij}^1, and Ψ_{ij}^2 are given in Eq. (37) shown in Box I. LMIs (55) would be guaranteed if Condition (35) is satisfied. Consequently, the theorem is proved.■

Remark 3. The suggested methods in Theorem 1 employ a simple technique to convert Nonlinear Inequalities (50) and (55) into Linear Inequalities (34) and (35). This technique has also been used in Refs. [48,49]. However, other suggested algorithms such as the mentioned technique in [50] can be utilized.

Remark 4. Theorem 1 proposes the LPV Controller (40) which requires α_i in real time among the measured parameters. In case the number of parameters is large, finding a closed formula to derive α_i from the parameters is difficult; however, an efficient algorithm has been proposed to calculate α_i in [51]. Therefore, this issue is not considered a limiting problem in Theorem 1.

Theorem 1 presents the gain-scheduled Controller (40) for the LPV system (Eq. (1)) obtained by the interpolation of multiple fixed static controllers in every vertex. However, one fixed controller can also be designed for the LPV system as the following corollary of Theorem 1.

Corollary 1. If the design of one fixed controller is desired, the parameter vector must be considered as an uncertain vector. According to the LPV controller (Eq. (39)) and Inequalities (34) and (35), if the same controllers are reconsidered in every vertex, one fixed controller, considering $Y_i = Y$, can be concluded if and only if LMIs (34) and (35) are feasible.

Corollary 1 is employed to calculate a fixed controller that enjoys simple implementation. However, in case the range of the parameters is large or the high performance is preferred, LMIs (34) and (35) may be infeasible. Equivalently, a fixed controller does not exist. In this situation, the gain-scheduled controller can be designed using Theorem 1.

5. The standard three-loop autopilot design for a pursuit

In this section, a standard three-loop autopilot is proposed to track commanded acceleration by considering the nonlinear tail-controlled pursuit model given by Nichols et al. [47]. The pursuit LPV model in Section 3 is employed so that the state feedback problem can be used in three-loop autopilot design using Theorem 1. Furthermore, to provide a reasonably realistic Mach profile in the next simulation results, Mach number is considered an exogenous signal by:

$$\dot{M}(t) = \frac{1}{\nu_s}\Big[-\left|A_z(t)\right|\sin\left(\left|\alpha(t)\right|\right) + A_x M^2(t)$$
$$\cos\left(\alpha(t)\right)\Big], \quad M(0) = M_0, \tag{56}$$

where A_x is proportional to the drag coefficient and its value can be found in Appendix B. In this section, at first, one fixed autopilot is designed through Corollary 1. By assuming Mach number and the angle of attack ranges as:

$$-20^\circ \leq \alpha(t) \leq 20^\circ, \quad 1 \leq M(t) \leq 2.5, \tag{57}$$

and considering Eq. (31), the range of the parameters θ_1 and θ_2 through a linear search for all possible values of Eq. (57) would be as follows:

$$-2.47 \leq \theta_1 \leq -0.131, \ 1 \leq \theta_2 \leq 6.25. \tag{58}$$

Furthermore, the augmented state-feedback structure is proposed in Figure 5 to design the autopilot where:

$$w(t) = [A_{zc}, Noise, Disturbabce], \quad z_\infty(t) = [z_e, z_u],$$

$$z_2(t) = z_e,$$

and the weighting functions are selected based on classical H_∞ synthesis as follows:

$$W_e = 0.5, \ \ W_n = 0.1, \ \ W_d = 0.1, \ \ W_u = 1.5. \tag{59}$$

The weighting W_e determines the desired speed required for tracking the problem and steady-state error of the closed-loop system. Preferably, W_e should be selected large, but it is quite impossible because the open-loop pursuit system is a non-minimum phase [52]. Therefore, this weight is set large enough to 0.5. The weights W_n and W_d are selected for robustness requirements on the measured noise and the input disturbance to a maximum amplitude of 0.1, respectively. The weight W_u imposes constraints on the control deflection to limit the actuator fin angle smaller than 40 degrees.

Now, the desired area in the complex plane is given by:

$$\mathrm{Re}\{z\} \leq -0.35, \quad \mathrm{Re}\{z\} \geq -100, x.$$

$$\tan(65) < -|y|. \tag{60}$$

Condition (60) limits the closed-loop poles to ensure a minimum decay rate of –0.35, maximum decay rate of –100, and minimum damping ratio of $\xi = \cos(65) = 0.43$. Based on Corollary 1, first, one fixed autopilot is obtained by solving LMIs (34) and (35) for the flight envelope (Inequalities (58)). The autopilot can guarantee the quadratic performance index $\gamma = 1.36$.

$$K = \begin{bmatrix} K_\alpha & K_q & K_z \end{bmatrix} = \begin{bmatrix} 7.02 & 1.23 & 0.82 \end{bmatrix}. \tag{61}$$

If the gain-scheduled autopilot considering the time-domain (60) is designed by solving LMIs (34) and (35) for the flight envelope (Eq. (57)), four fixed autopilots that ensure higher quadratic performance $\gamma = 1.02$ can be obtained as follows:

$$K_1 = \begin{bmatrix} K_{\alpha_1} & K_{q_1} & K_{z_1} \end{bmatrix} = \begin{bmatrix} 07.16 & 1.26 & 1.27 \end{bmatrix},$$

$$K_2 = \begin{bmatrix} K_{\alpha_2} & K_{q_2} & K_{z_2} \end{bmatrix} = \begin{bmatrix} 12.26 & 1.26 & 1.37 \end{bmatrix},$$

$$K_3 = \begin{bmatrix} K_{\alpha_3} & K_{q_3} & K_{z_3} \end{bmatrix} = \begin{bmatrix} 06.99 & 1.19 & 0.76 \end{bmatrix},$$

$$K_4 = \begin{bmatrix} K_{\alpha_4} & K_{q_4} & K_{z_4} \end{bmatrix} = \begin{bmatrix} 07.41 & 0.96 & 0.80 \end{bmatrix}. \tag{62}$$

Therefore, by determining the vertex numbers, as presented in Table 2, and applying Controllers (62), LPV Controller (40) is derived by interpolation gains in real time. In the following, a closed formula is proposed to calculate these interpolation gains. By defining:

$$x = \frac{\max(\theta_1) - \theta_1}{\max(\theta_1) - \min(\theta_1)},$$

$$y = \frac{\max(\theta_2) - \theta_2}{\max(\theta_2) - \min(\theta_2)}, \tag{63}$$

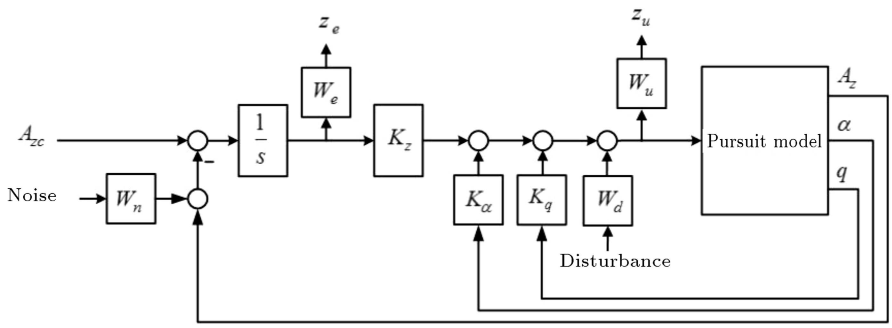

Figure 5. The proposed augmented structure for a mixed H_2/H_∞ design with time domain constraints.

Table 2. Vertex values of the parameter box (Eq. (58)).

Parameter vector	Vertex 1	Vertex 2	Vertex 3	Vertex 4
$[\theta_1\ \theta_2]$	$[-2.47\ 1]$	$[-0.131\ 1]$	$[-2.47\ 6.25]$	$[-0.131\ 6.25]$

the coefficients α_i are selected using the following equations so that the polytope condition (Eq. (4)) on $\theta(t) = \begin{bmatrix}\theta_1 & \theta_2\end{bmatrix}$ is satisfied.

$$\alpha_1 = xy, \qquad \alpha_2 = (1-x)\,y, \qquad \alpha_3 = (1-y)\,x,$$
$$\alpha_4 = (1-x)(1-y). \tag{64}$$

Figures 6–8 present the simulation results of using the autopilot gains (Eqs. (61) and (62)) and the interpolation gains (Eq. (64)), assuming that $Noise = 0.1\sin(100\pi t)$, $M_0 = 2.5$, and the disturbance profile shown in Figure 9.

As observed in Figure 6, the tail-controller pursuit model is a non-minimum phase system. Controlling such systems is difficult. However, the proposed method satisfies a good performance in acceleration tracking capability with sufficiently fast time response, noise/disturbance attenuation, proper amplitude of angle of attack and angular velocity, and tail deflection. Furthermore, because the time-domain and frequency-domain constraints are similar for both fixed and multiple autopilots and LMIs (34) and (35) are feasible for both of them, the time-domain of the closed-loop responses will be close, as seen in Figures 6 to 8. Nevertheless, the performance γ of multiple controllers is smaller than the other ones. Furthermore, to check satisfaction of the pole placement constraints (Eq. (60)), the closed-loop system should be considered as a LTI system. Therefore, the closed-loop pursuit system has been simulated with autopilot gains (Eqs. (61) and (62)) by considering the scenario given in Figure 6. The location of the closed-loop poles is plotted in Figure 10 for 70 fixed points.

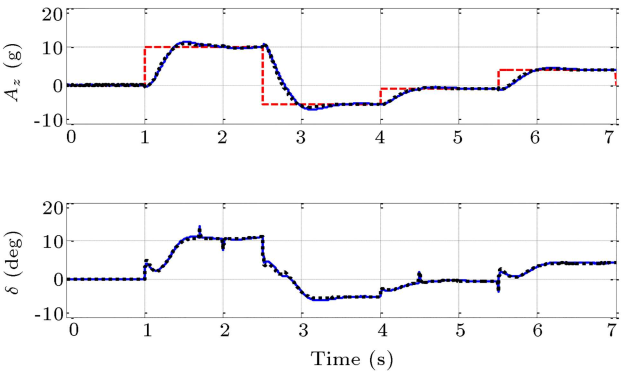

Figure 6. The acceleration response and tail deflection (solid line: fixed autopilot; dashed line: gain scheduled autopilot).

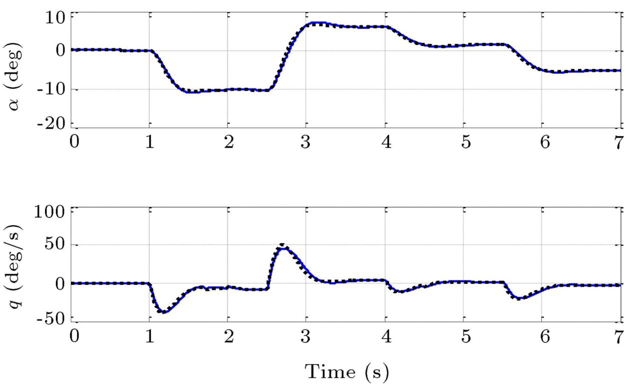

Figure 7. The angle of attack and the angular velocity (solid line: fixed autopilot; dashed line: gain scheduled autopilot).

Figure 10 validates the pole placement constraints given in Eq. (60) by Autopilots (61) and (62). However, a fixed autopilot cannot be designed if the desired area in the complex plane is selected as:

$$\mathrm{Re}\{z\} \le -1.25, \quad \mathrm{Re}\{z\} \ge -85,$$
$$x.\tan(65) < -|y|. \tag{65}$$

Equivalently, LMIs (34) and (35) will be infeasible. However, the gain-scheduled controller satisfies the performance index $\gamma = 1.5$ by the following controllers.

$$K_1 = \begin{bmatrix}K_{\alpha_1} & K_{q_1} & K_{z_1}\end{bmatrix} = \begin{bmatrix}06.56 & 1.15 & 1.70\end{bmatrix},$$
$$K_2 = \begin{bmatrix}K_{\alpha_2} & K_{q_2} & K_{z_2}\end{bmatrix} = \begin{bmatrix}15.56 & 1.89 & 2.29\end{bmatrix},$$
$$K_3 = \begin{bmatrix}K_{\alpha_3} & K_{q_3} & K_{z_3}\end{bmatrix} = \begin{bmatrix}09.40 & 1.06 & 1.06\end{bmatrix},$$
$$K_4 = \begin{bmatrix}K_{\alpha_4} & K_{q_4} & K_{z_4}\end{bmatrix} = \begin{bmatrix}07.04 & 0.60 & 0.90\end{bmatrix}. \tag{66}$$

Consequently, the gain-scheduled controller is more achievable than the fixed one. A mixed H_2/H_∞ pitch autopilot was designed using the LPV control techniques in [51]. In [51], the plant was characterized by a Linear Fractional Transformation (LFT) representation. Therefore, a multi-channel LFT/LPV control method was applied. By considering Model (14), the augmented LFT/LPV interconnection shown in Figure 11 was chosen (the value of parameters in Figure 11 was given in [51]). Furthermore, the system parameter $\alpha(t)$ was used for the interpolation procedure. Finally, the full-order controller $F_L(K(s), \Delta_K(\theta_\alpha))$ guarantees the H_∞ and H_2 performance indices 3 and 15, respectively. However, the proposed static autopilot in Eq. (62) guarantees the value of 1.02 for both H_∞ performance and H_2 performance.

To make a comparison between the proposed autopilot and the suggested controller in [51] in the time-domain, the pole-placement constraints (65) were defined in Eq. (67) to track step commands with the time constant no more than 0.35 second, maximum overshoot of 10%, and a steady-state error less than 1%. These criteria were considered in [51]. Consequently, they can be compared in the time domain. If the following area in the complex plane is selected:

$$\mathrm{Re}\{z\} \le -2.25, \quad \mathrm{Re}\{z\} \ge -158,$$
$$x.\tan(65) < -|y|, \tag{67}$$

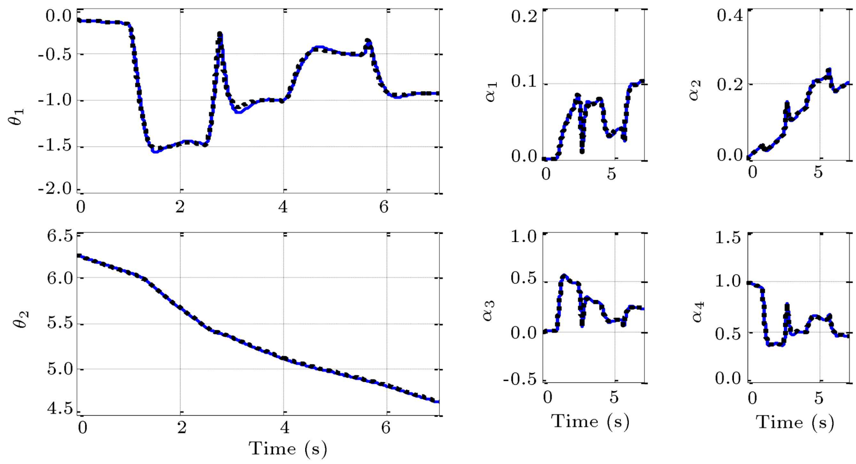

Figure 8. The time-varying parameters (solid line: fixed autopilot; dashed line: gain scheduled autopilot).

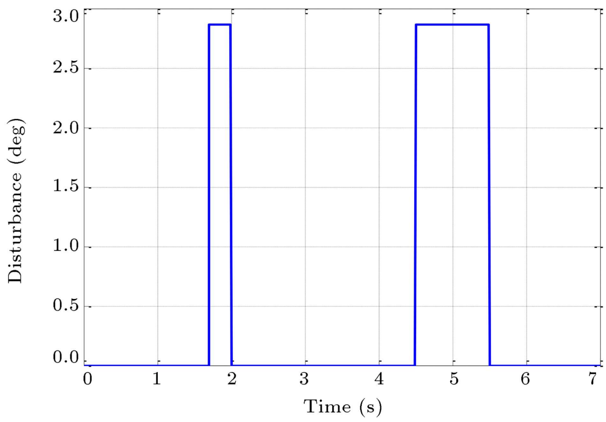

Figure 9. The disturbance profile.

the following autopilot guarantees the robust H_2/H_∞ index $\gamma = 2.99$:

$$K_1 = \begin{bmatrix} K_{\alpha_1} & K_{q_1} & K_{z_1} \end{bmatrix} = \begin{bmatrix} 37.46 & 2.78 & 9.59 \end{bmatrix},$$

$$K_2 = \begin{bmatrix} K_{\alpha_2} & K_{q_2} & K_{z_2} \end{bmatrix} = \begin{bmatrix} 39.94 & 2.79 & 9.84 \end{bmatrix},$$

$$K_3 = \begin{bmatrix} K_{\alpha_3} & K_{q_3} & K_{z_3} \end{bmatrix} = \begin{bmatrix} 18.91 & 1.31 & 3.34 \end{bmatrix},$$

$$K_4 = \begin{bmatrix} K_{\alpha_4} & K_{q_4} & K_{z_4} \end{bmatrix} = \begin{bmatrix} 17.71 & 1.09 & 3.83 \end{bmatrix}. \quad (68)$$

Figures 12 and 13 present the step response while applying Autopilot (68) and the suggested autopilot in [51].

As shown in Figures 12 and 13, the proposed static method had a better time-domain performance than the method suggested in [51]. In addition, the design procedure suggested in [51] was more difficult than the proposed method. As a result, the proposed method can ensure better performance in the time domain and frequency domain as well as in both simpler design procedure and static topology.

6. Conclusion

In this paper, the design problem of standard three-loop autopilot was converted into a standard static state-feedback control problem. Furthermore, a theorem based on Linear Matrix Inequality (LMI) approach was proposed that could guarantee both the mixed H_2/H_∞ performance and regional pole placement constraints for the Linear Parameter Varing (LPV)

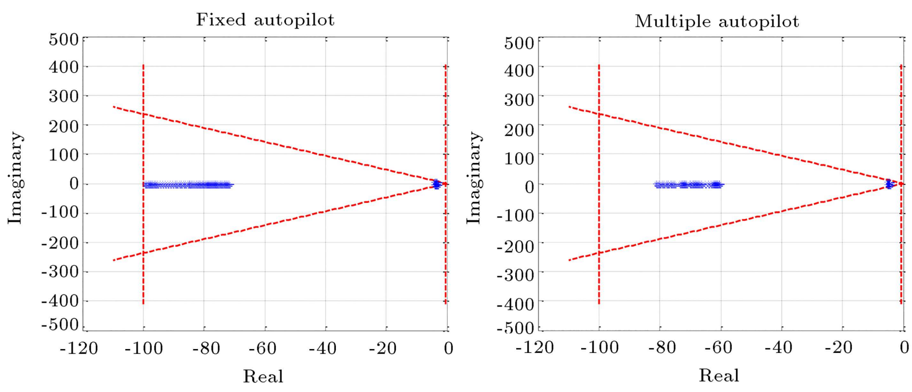

Figure 10. The validation of time domain constraints (*:closed loop poles; dashed line: time domain constraints).

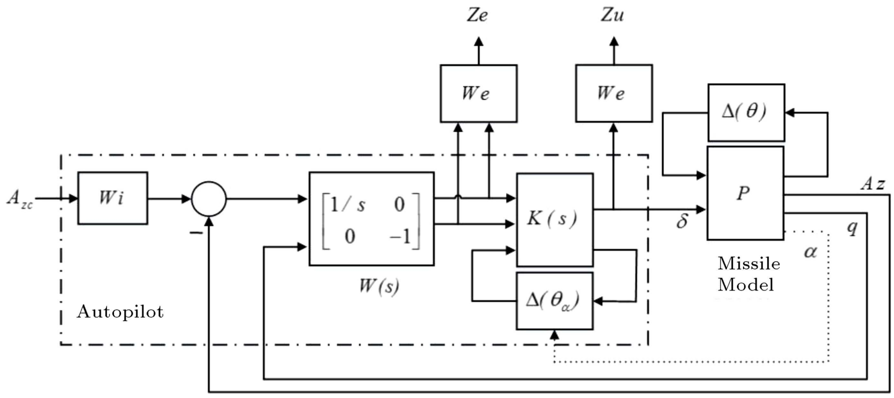

Figure 11. Control structure and synthesis interconnection [51].

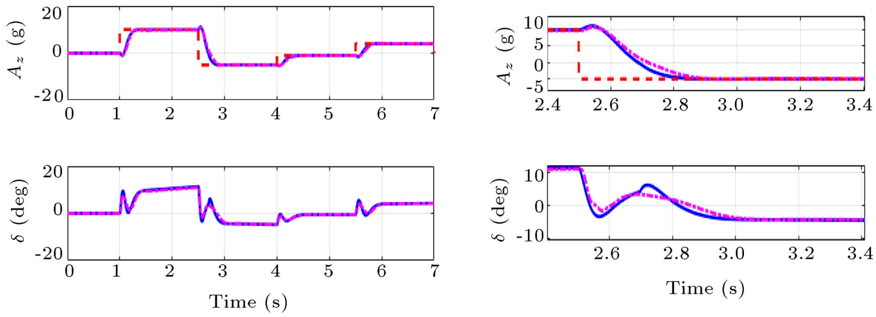

Figure 12. The acceleration response and tail deflection parameters (solid line: Autopilot (66); dashed line: suggested autopilot in [51].

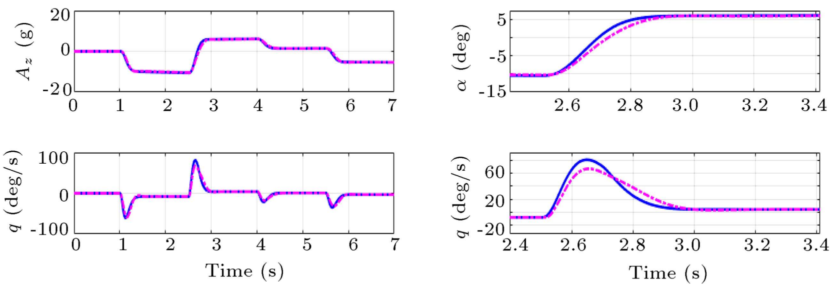

Figure 13. The angle of attack and the angular velocity (solid line: Autopilot (66); dashed line: suggested autopilot in [51]).

systems. The simulation results showed that in case the range of varying parameters was not large, a fixed static autopilot could be used for guaranteeing the mixed H_2/H_∞ performance and desired time-domain constraints. However, when the range of the parameters was notably large, a gain-scheduled autopilot would be required.

References

1. Jackson, P.B. "Overview of missile flight control systems", *John Hopkins APL Technical Digest*, **29**(1), pp. 9–24 (2010).
2. Li, S. and Yang, J. "Robust autopilot design for bank-to-turn missiles using disturbance observers", *IEEE Transactions on Aerospace and Electronic Systems*, **49**(1), pp. 558–579 (2013).
3. Statement, I.P. "Pitch autopilot design for agile missiles with uncertain aerodynamic coefficients", *IEEE Transactions on Aerospace and Electronic Systems on Aerospace and Electronic Systems*, **49**(2), pp. 907–914 (2013).
4. Reichert, R.T. "Dynamic scheduling of modern-robust-control autopilot designs for missiles", *IEEE Control Systems*, **12**(5), pp. 35–42 (1992).
5. Biannic, J.M. and Apkarian, P. "Missile autopilot design via a modified LPV synthesis technique", *Aerospace Science and Technology*, **3**(3), pp. 153–160 (1999).

6. Theodoulis, S., Seve, F., and Wernert, P. "Robust gain-scheduled autopilot design for spin-stabilized projectiles with a course-correction fuze", *Aerospace Science and Technology*, **42**, pp. 477–489 (2015).

7. Shen, Y., Yu, J., Luo, G., et al. "Missile autopilot design based on robust LPV control", *Journal of Systems Engineering and Electronics*, **28**(3), pp. 536–545 (2017).

8. Leith, D.J., Tsourdos, A., White, B.A., et al. "Application of velocity-based gain-scheduling to lateral autopilot design for an agile missile", *Control Engineering Practice,* **9**(10), pp. 1079–1093 (2001).

9. Mohammadpour, J. and Scherer, C.W., *Control of Linear Parameter Varying Systems with Applications*, New York: Springer (2012).

10. Shamma, M.A.J. "Guaranteed properties of gain scheduled control for linear parameter-varying plants", *Automatica*, **27**(3), pp. 559–564 (1991).

11. Vesely , V. and Ilka, A. "Gain-scheduled PID controller design", *Journal of Process Control*, **23**(8), pp. 1141–1148 (2013).

12. Ilka, A. and Vesely, V. "Discrete gain-scheduled controller design: Variable weighting approach", *Journal of Electrical Engineering*, **65**(2), pp. 116–120 (2014).

13. Guo, Z., Yao, X., and Zhang, X. "Robust gain scheduled longitudinal autopilot design for rockets during the sustaining phase", *Proceedings of the Institution of Mechanical Engineers. Part I: Journal of Systems and Control Engineering*, **230**(10), pp. 1154–1163 (2016).

14. Lhachemi, H., Saussié, D., and Zhu, G. "Handling hidden coupling terms in gain-scheduling control design: Application to a pitch-axis missile autopilot", *AIAA Guidance, Navigation, and Control Conference*, pp. 1–21 (2016).

15. Xiaofeng, S. and Yingmin, J. "Self-scheduled robust decoupling control with H_∞ performance of hypersonic vehicles", *Systems & Control Letters*, **70**, pp. 38–48 (2014).

16. Yang , S.M. and Huang, N.H. "Application of H_∞ control to pitch autopilot of missiles", *IEEE Transactions on Aerospace and Electronic Systems IEEE*, **32**(1), pp. 426–433 (1996).

17. Veenman, J. and Scherer, C.W. "A synthesis framework for robust gain-scheduling controllers", *Automatica*, **50**(11), pp. 2799–2812 (2014).

18. Behrouz, H., Mohammadzaman, I., and Mohammadi, A. "Robust static output feedback design with pole placement constraints for linear systems with polytopic uncertainties", *Transactions of the Institute of Measurement and Control*, pp. 1–11 (2019).

19. Hoffmann, C. and Werner, H. "A survey of linear parameter-varying control applications validated by experiments or high-fidelity simulations", *IEEE Transactions on Automatic Control Systems Technology,* **23**(2), pp. 416–433 (2015).

20. Li, T., Zhang, S., Yang , H., et al. "Robust missile longitudinal autopilot design based on equivalent-input-disturbance and generalized extended state observer approach", *Proceedings of the Institution of Mechanical Engineers, Part G: Journal of Aerospace Engineering,* **229**(6), pp. 1025–1042 (2015).

21. Kurkcu, B. and Kasnakoglu, C. "Robust autopilot design based on a disturbance/uncertainty /coupling estimator", *IEEE Transactions on Control Systems Technology*, **27**(6), pp. 2622–2629 (2018).

22. Dong, Y., Li, J., and Li, T. "Generalized extended state observer-based Ȟ221e control design for a missile longitudinal autopilot", *Proceedings of the Institution of Mechanical Engineers, Part G: Journal of Aerospace Engineering*, **230**(12), pp. 2162–2178 (2016).

23. Chen, B.S. and Zhang, W. "Stochastic H_2/H_∞ control with state dependent noise", *IEEE Transactions on Automatic Control*, **49**(1), pp. 45–57 (2004).

24. Ibrir, S. and Sabir, A. "Dynamic output stabilization and tracking of uncertain linear systems with mixed H_2/H_∞ performance", *11th Conference on Industrial Electronics and Applications (ICIEA)* (2016).

25. Lien, C.H., Yu, K.W., Lin, Y.F., et al. "Robust reliable H_∞ control for uncertain nonlinear systems via LMI approach", *Applied Mathematics and Computation*, **198**(1), pp. 453–462 (2008).

26. Prempain, E. and Postlethwaite, I. "L2 and H2 performance analysis and gain-scheduling synthesis for parameter-dependent system", *Automatica*, **44**(8), pp. 2081–2089 (2008).

27. Qingjiang , H., Sijun, Y., Yan, L., et al. "An enhanced LMI approach for mixed $H2/H_\infty$ flight tracking control", *Chinese Journal of Aeronautics*, **24**, pp. 324–328 (2011).

28. Rotondo, D., Ejjari, F., and Puig, V. "Robust state-feedback control of uncertain LPV systems: An LMI-based approach", *Journal of the Franklin Institute*, **351**(5), pp. 2781–2803 (2014).

29. Scherer, C.W. "An efficient solution to multi-objective control problems with LMI objectives", *Systems & Control Letters,* **40**(1), pp. 43–57 (2000).

30. Magni, J.F. "Multimodel eigenstructure assignment in flight-control design", *Aerospace Science and Technology,* **3**(3), pp. 141–151 (1999).

31. Lee, C.H., Shin, M.H., and Chung, M.J. "A design of gain-scheduled control for a linear parameter varying system: an application to flight control", *Control Engineering Practice*, **9**(1), pp. 11–21 (2011).

32. Lhachemi, H., Saussie, D., and Zhu, G. "Explicit hidden coupling terms handling in gain-scheduling control design via eigenstructure assignment", *Control Engineering Practice*, **58**, pp. 1–11 (2017).

33. Wang, H., Lin, D., Wang , J., et al. "An analytical design method for the missile two-loop acceleration autopilot", *International Computer Science Conference (ICSC)* (2012).

34. Lee, C.H., Jun, B.E., and Lee, J.I. "Connections between linear and nonlinear missile autopilots via three-loop topology", *Journal of Guidance, Control, and Dynamics*, **39**(6), pp. 1424–1430 (2016).

35. Nesline, W. and Zarchan, P. "Robust instrumentation configurations for homing missile flight control", *AIAA Guidance, Navigation, and Control*, pp. 209–219 (1980).

36. Mohamed, E.M. and Yan, L. "Design and comparison of two-loop with PI and three-loop autopilot for static unstable missile", *International Journal of Computer and Electrical Engineering*, **8**(1), pp. 1–11 (2016).

37. Kim, J.H. and Whang, I.H. "Augmented three-loop autopilot structure based on mixed-sensitivity H_∞ optimization", *Journal of Guidance, Control, and Dynamics,* **41**(3), pp. 748–753 (2018).

38. Abd-Elatif, M.A., Qian, L., and Bo, Y. "Optimization of three-loop missile autopilot gain under crossover frequency constraint", *Defence Technology,* **12**(1), pp. 32–38 (2016).

39. Mracek, C.P. and Ridgely, D.B. "Missile longitudinal autopilots: comparison of multiple three loop topologies", *AIAA Guidance, Navigation, and Control Conference and Exhibit*, San Francisco, pp. 917–928 (2005).

40. Defu, L., Junfang, F., Zaikang, Q., et al. "Analysis and improvement of missile three-loop autopilots", *System Engineering Electronic*, **20**(4), pp. 844–851 (2009).

41. Qiu, W., Li, X.Q., and Kang, Q.Z. "Pole placement design with open-loop crossover frequency constraint for three-loop autopilot", *System Engineering Electronic* (in China), **2** (2009).

42. Zhou, K., *Essentials of Robust Control*, Prentice-Hall (1998).

43. Apkarian, P., Noll, D., and Rondepierre, A. "Mixed H_2/H_∞ control via nonsmooth optimization", *SIAM Journal on Control and Optimization*, **47**(3), pp. 1516–1546 (2008).

44. Apkarian, P., Gahinets, P., and Becker, G. "Self-scheduled H_∞ control of linear parameter-varying systems: a design example", *Automatica*, **31**(9), pp. 1251–1261 (1995).

45. Scherer, C. and Weiland, S. "Linear matrix inequalities in control", *Lecture Notes, Dutch Institute for Systems and Control*, Delft, The Netherlands (2000).

46. Zipfel, P.H. "Modeling and simulation of aerospace vehicle dynamics", In *AIAA*, Second Edition (2007).

47. Nichols, R.A., Reichert, R.T., and Rugh, W.J. "Gain scheduling for H-infinity controllers: a flight control example", *IEEE Transactions on Control Systems Technology*, **1**(2), pp. 69–79 (1993).

48. Dong, J. and Yang, G.-H. "Robust static output feedback control synthesis for linear continues systems with polytopic uncertainties", *Automatica*, **49**(6), pp. 1821–1829 (2013).

49. Chang, X.-H., Park, J.H., and Zhou, J. "Robust static output feedback H_∞ control design for linear systems with polytopic uncertainties", *Systems & Control Letters*, **85**, pp. 23–32 (2015).

50. Ramos, D.C.W. and Peres, P.L.D. "An LMI condition for the robust stability of uncertain continuous-time linear systems", *IEEE Transactions on Automatic Control*, **47**(4), pp. 675–678 (2002).

51. Pellanda, P.C., Apkarian, P., and Tuan, H.D. "Missile autopilot design via a multi-channel LFT / LPV control method", *International Journal of Nonlinear and Robust Control*, **12**(1), pp. 1–20 (2002).

52. Zhou, K., Doyle, J.C., and Glover, K., *Robust and Optimal Control*, In Prentice Hall, New Jersey (1996).

Appendix A [45]

The LTI system $\dot{x}(t) = Ax(t)$ is asymptotically stable if and only if all eigenvalues of A lie in the left half of the complex plane, $\mathbb{C}^-$. By defining a stability region as a subset $\mathbb{C}_{stability} \subseteq \mathbb{C}$ if $\lambda \in \mathbb{C}_{stability}$ and considering $\mathbb{C}_{stability}$ as convex, the typical examples of common region stability set are summarized in Table A.1.

Appendix B [47]

The details of the model parameters have been shown in Table B.1.

Table A.1. Time-domain characteristics using Linear Matrix Inequalities (LMIs).

$\mathbb{C}_{stability}$	**Region**	
$\mathbb{C}^-$	Open left half of the complex plane	$P = \begin{pmatrix} 0 & 1 \\ 1 & 0 \end{pmatrix}$
$\mathbb{C}$	No stability requirement	$P = \begin{pmatrix} -1 & 0 \\ 0 & 0 \end{pmatrix}$
$\{s \in \mathbb{C} \mid \mathrm{Re}(s) < -\alpha\}$	Guaranteed damping	$P = \begin{pmatrix} 2\alpha & 1 \\ 1 & 0 \end{pmatrix}$

Table A.1. Time-domain characteristics using Linear Matrix Inequalities (LMIs) (continued).

$\mathbb{C}_{stability}$	Region	
$\{s \in \mathbb{C} \mid \lvert s \rvert < r\}$	circle centered at origin	$P = \begin{pmatrix} -r^2 & 0 \\ 0 & 1 \end{pmatrix}$
$\{s \in \mathbb{C} \mid \alpha_1 \prec \mathrm{Re}(s) < \alpha_2\}$	Vertical strip	$P = \begin{pmatrix} 2\alpha_1 & 0 & -1 & 0 \\ 0 & -2\alpha_2 & 0 & 1 \\ -1 & 0 & 0 & 0 \\ 0 & 1 & 0 & 0 \end{pmatrix}$
$\{s \in \mathbb{C} \mid \mathrm{Re}(s)\tan(\theta) < -\lvert \mathrm{Im}(s) \rvert\}$	Conic stability region	$P = \begin{pmatrix} 0 & 0 & \sin(\theta) & \cos(\theta) \\ 0 & 0 & -\cos(\theta) & \sin(\theta) \\ \sin(\theta) & -\cos(\theta) & 0 & 0 \\ \cos(\theta) & \sin(\theta) & 0 & 0 \end{pmatrix}$

Table B.1. Details of the pitch-axis pursuit model.

$K_\alpha = 0.7P_0S/m\,\nu_s$	
$K_q = 0.7P_0Sd/Iy$	
$K_z = 0.7P_0S/m$	
$P_0 = 973.3$ l bs/ft^2	Static pressure at 20,000 ft
$S = 0.44$ ft^2	Surface area
$m = 13.98$ slugs	Mass
$\nu_s = 1036.4$ ft/sec	Speed of sound at 20,000 ft
$d = 0.75\,ft$	Diameter
$I_y = 182.5$ slug.ft^2	Pitch moment of inertia
$C_a = -0.3$	Drag coefficient
$A_x = 0.7P_0SC_a/m$	
$a_n = 0.000103$ deg^{-3}	$a_m = 0.000215$ deg^{-3}
$b_n = -0.00945$ deg^{-2}	$b_m = -0.0195$ deg^{-2}
$c_n = -0.1696$ deg^{-1}	$c_m = 0.051$ deg^{-1}
$d_n = -0.034$ deg^{-1}	$d_m = -0.206$ deg^{-1}

Biographies

Hadi Behrouz is currently pursuing the PhD degree in Control Engineering at Malek Ashtar University of Technology, Tehran, Iran. His research interests include robust and multi-objective control and LMI optimization.

Iman Mohammadzaman is an Assistant Professor at Electrical Engineering Department, Malek Ashtar University of Technology, Tehran, Iran. His research interests include robust control, nonlinear control, and LMI optimization.

Ali Mohammadi is an Assistant Professor at Electrical Engineering Department, Malek Ashtar University of Technology, Tehran, Iran. His research interests include estimation, signal processing, and control of LPV systems.